

Detection of Broken Rotor Bars in the Squirrel Cage Induction Motors

¹Tahar Bahi, ¹Amel Ourici, ²George Barakat, ¹Mohamed Benouaret

¹Faculty of Sciences Engineering, Badji Mokhtar University, BP.12, Sidi Amar, Annaba, Algeria

²GREAH, University du Havre, BP 540, 76058 LE HAVRE, France

Abstract: This study deals with a global method enabling the simulation for the detection of rotor cage faults in operating three phase induction motors. This method is based on the coupled magnetic circuit theory and it presents an application regarding possibilities of predicting the performance in electrical machine. The system of differential equations describing the induction motor in presence of rotor faults is given. The machine inductances are calculated by means of the magnetic energy stored in the airgap. This task is performed by the use of the winding functions method and a previously developed airgap permeance analytical model. Finally, some simulation results illustrate the proposed global method in the case of the broken rotor bars faults of induction motors.

Key words: Induction motors, winding functions, broken bar, faults diagnosis

INTRODUCTION

Induction motors play an important role in the safe and efficient operation of industrial plants. Usually they are designed for thirty years faults-free lifetime^[1], but most of them are not available at all times. The squirrel cage induction motor is one of the most used machines in industrial application. An important number of these motors is working at critical points of the industry processes, which can result faults in different parts of the motor^[2]. Unfortunately, the electrical machines protection system cannot avoid the presence of these faults and their direct affect on electrical machines, since the protection apparatus will respond only at the final stage of the fault^[3].

Hence, for several years, an important number of papers dealing with faulty induction machines have been published. Amongst the various diagnostic methods used recently and mainly those using a data base containing information related to the various faults and issued from the spectral analysis of several motor quantities such as stator currents, instantaneous stator power, electromagnetic torque^[4-6], etc... The current stator approach requires only a current sensor, able to give a clear picture of the picture of the stator current.

Therefore, the availability of a simulation model in the study of faulty machine becomes attractive. Then, the objective of this study is to develop an accurate model which is capable of predicting the performance of induction machines under rotor faults. The proposed model is based on a coupled magnetic circuit approach and the differential equations system governing the

induction machine behavior is given. The expressions of the different magnetizing inductances and mutual inductances are derived from the stored magnetic energy in the air gap unlike the widely used method based on the air gap flux across the windings^[7]. The stored magnetic energy in the air gap is calculated using the winding functions theory^[8] and a previously developed doubly slotted air gap permeance model^[9]. The rotor bar skew is also taken into account in the inductances calculation. The rotor bar resistances as well as the rotor end ring resistances depend on the rotor speed with conventional formulas.

Finally, some simulation results illustrate the proposed model in the case of healthy machine and one broken rotor bars.

MODELLING OF INDUCTION MACHINES

A squirrel cage three phase motor is considered, its rotor is composed of q isolated bars, uniformly distributed on the rotor surface and short circuited with two rings.

The rotor is described in the terms of loops as shown in Fig. 1. Rotor loop currents are defined as the currents flowing in loops comprising two adjacent rotor bars and the portions of end ring joining them. Each rotor bar and end ring segment are characterized by a resistance and inductance. For an q bars-rotor, three-phase squirrel cage induction motor, $q + 3$ windings couple with each other through the air gap flux.

In order to study the motor performance during a faulty rotor, a model is being used in which the cage of the rotor is equivalent to a mesh circuit. The differential

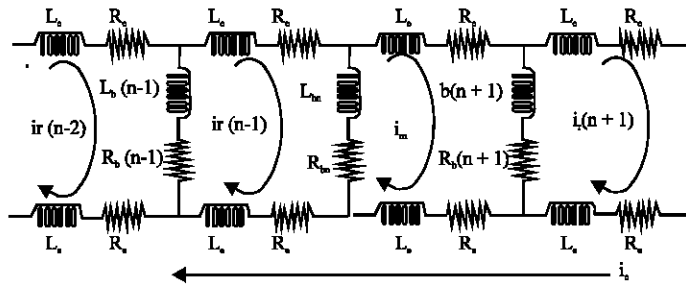


Fig. 1: Rotor cage equivalent circuit

equations system of the induction machine in the healthy case and the broken rotor bars will be given in the case of delta connected stator phases. Usually, the neutral line of the stator phases of induction machines is not connected and the star connected case equations are obtained from the delta connected case ones by replacing one phase current by minus the sum of the other phase's currents. The number of differentials equations obtained is equal to number of bars plus one^[10].

For the case of Healthy Machine, the model considered in replacing the \$q\$ bars squirrel cage by an equivalent circuit containing \$q + 1\$ magnetically coupled meshes. The current in each mesh of the rotor cage is an independent variable. Classical assumptions are to be considered such as infinite permeability of iron as well as no inter-bar currents. With these assumptions, the system of differential equations describing the behavior of induction machine with \$m\$ stator phases and \$q\$ rotor bars can be written in vector-matrix form and in a compact manner as follows^[11,12].

$$\begin{cases} \frac{d}{dt} [I] = -[L]^{-1} \left([R] + \Omega \frac{d[L]}{d\theta} \right) [I] + [L]^{-1} [V] \\ \frac{d\Omega}{dt} = \frac{1}{2J} [I]^t \left\{ \frac{d[L]}{d\theta} \right\} [I] - \frac{f}{J} \Omega - \frac{1}{J} T_L \\ \frac{d\theta}{dt} = \Omega \end{cases} \quad (1)$$

Where:

\$[R]\$ and \$[L]\$ are the resistances and the inductances matrices respectively;

$$[R] = \begin{bmatrix} [R_s] & [0] \\ [0] & [R_r] \end{bmatrix} \quad (2)$$

$$[L] = \begin{bmatrix} [L_{ss}] & [L_{sr}] \\ [L_{rs}] & [L_{rr}] \end{bmatrix} \quad (3)$$

$$[R_s] = \begin{bmatrix} R_{s1} & 0 & \dots & \dots & \dots & 0 \\ 0 & R_{s2} & 0 & \dots & \dots & 0 \\ \dots & \dots & \dots & \dots & \dots & \dots \\ \dots & \dots & \dots & \dots & \dots & \dots \\ \dots & \dots & \dots & \dots & R_{sm-1} & 0 \\ 0 & \dots & \dots & \dots & \dots & R_{sm} \end{bmatrix} \quad (4)$$

$$[L_{ss}] = \begin{bmatrix} L_{s1s1} & L_{s1s2} & \dots & \dots & \dots & L_{s1sm} \\ L_{s2s1} & L_{s2s2} & \dots & \dots & \dots & L_{s2sm} \\ \dots & \dots & \dots & \dots & \dots & \dots \\ \dots & \dots & \dots & \dots & \dots & \dots \\ L_{sm-1s1} & \dots & \dots & \dots & \dots & L_{sm-1sm} \\ L_{sm-1s1} & \dots & \dots & \dots & \dots & L_{sm-1sm} \end{bmatrix} \quad (5)$$

$$[L_{sr}] = \begin{bmatrix} L_{s1r1} & L_{s1r2} & \dots & \dots & \dots & L_{s1rq} \\ L_{s2r1} & L_{s2r2} & \dots & \dots & \dots & L_{s2rq} \\ \dots & \dots & \dots & \dots & \dots & \dots \\ \dots & \dots & \dots & \dots & \dots & \dots \\ L_{sm-1r1} & \dots & \dots & \dots & \dots & L_{sm-1rq} \\ L_{smr1} & L_{smr2} & \dots & \dots & \dots & L_{smrm} \end{bmatrix} \quad (6)$$

\$[I]\$ and \$[V]\$ are the current and the voltages vectors.

With:

$$[V]^t = [V_s]^t [0]^t = [v_{s1} \ v_{s2} \ v_{s3} \ \dots \ v_{sm}]^t [0]^t \quad (7)$$

$$[I]^t = [I_s]^t [I_r]^t = [i_{r1} \ \dots \ i_{sm}]^t [i_{r1} \ \dots \ i_{rq} \ i_e]^t \quad (8)$$

\$T_L\$ is the load torque and \$J\$ is the inertia moment of the machine.

In addition, the calculation of all the relevant inductances for the induction machine is based on the winding functions^[10]. Their expressions were derived from the calculation of the air-gap flux embraced by the

windings. This method results to the use of the distribution function of the windings in the calculation of mutual inductances. In the exposed model, the calculation of inductances is derived from the magnetic energy stored in the air-gap. The mutual inductance between winding 'i' and winding 'j' is expressed by following formulae.

$$L_{ij}(\theta) = \frac{1}{\mu_0} \int_0^{L_{ax}} \int_0^{2\pi} F_{wi}(\theta, \theta_s, z) \cdot F_{wj}(\theta, \theta_s, z) e(\theta, \theta_s, z) P^2(\theta, \theta_s, z) R_{av}(\theta, \theta_s, z) d\theta_s \cdot dz \quad (9)$$

With the $R_{av}(\theta, \theta_s, z)$ is the average radius of the air-gap given by:

$$R_{av}(\theta, \theta_s, z) = R_r + e(\theta, \theta_s, z)/2 \quad (10)$$

Where:

- L_{ax} : is the effective airgap axial length;
- $e(\theta, \theta_s, z)$: is the effective air-gap function;
- $F_{wi}(\theta, \theta_s, z)$: is the winding functions of winding 'i';
- $F_{wj}(\theta, \theta_s, z)$: is the winding functions of winding 'j';
- And $P(\theta, \theta_s, z)$: is the airgap permeance function.

Broken rotor bars can be a serious problem with certain induction motors due to arduous duty cycles. Although broken rotor bars do not initially cause an induction motor to fail, there can be serious secondary effects. The fault mechanism can result in broken parts of the hitting the end winding. This can cause serious mechanical damage to the insulation and a consequential winding failure may follow, resulting in a costly repair and lost production^[13].

For the study of Broken Rotor Bars, the rotor cage is modeled by an equivalent circuit containing $q + 1$ magnetically coupled meshes. Practically, the rotor bars are numbered from 1 to q either a bar is broken or not and their state is saved (broken or healthy). In order to define the rotor meshes, one searches the first healthy bars which constitute the first bar of the first mesh. The following healthy bar is the second bar of the first mesh. The second and following rotor meshes are constructed in the same manner. Consequently, if mesh 'k' is constituted by bar 'i' and bar 'j' separated by n_{bb} consecutive broken bars, the resistance of mesh 'k' is given by:

$$R_k = 2.R_b + 2.(n_{bb} + 1).R_e \quad (11)$$

And the total inductance of mesh 'k' is:

$$L_{mkk} = L_{rkk} + 2.L_{\sigma b} + 2.(n_{bb} + 1).L_{\sigma e} \quad (12)$$

Where, L_{rkk} is the magnetizing inductance of the mesh 'k' given in^[11]. It is important to note that the winding function of a mesh is obtained by the summation of the winding functions of each of the two bars constituting the considered mesh. Also, the mutual inductance between mesh 'k' and the end ring become

$$L_{mke} = (n_{bb} + 1).L_{\sigma e} \quad (13)$$

Obviously, the new dimension of system (1) is obtained by subtracting the total number of broken bars from its dimension in the healthy case ($m + q + 1$). The mutual inductances between rotor meshes on one side and between rotor meshes and stator phases on the other side are calculated by means of expression (9) with the use of adequate winding functions for meshes containing broken bars.

In the same manner, the end rings are numbered from 1 to q either an end ring is broken or not and their state is saved (broken or healthy). When a broken end ring occurs, the corresponding cage mesh in the healthy case is included in the ring mesh. So, if n_{ber} designates an adequate number of broken end rings, the resistance of the ring mesh is expressed by:

$$R_{mr} = q.R_e + n_{ber}.R_b \quad (14)$$

The number n_{ber} must be determined by an adequate algorithm based on the different changes in the cage circuit induced by the broken end rings. A similar algorithm is used to determine the magnetizing and leakage inductances of the cage meshes and the ring mesh which total inductance is expressed by

$$L_{mee} = 2.L_{\sigma b} + 2.(n_{bb} + 1).L_{\sigma e} + \sum_k L_{rkk} \quad (15)$$

The L_{rkk} are the magnetizing inductances corresponding to the meshes containing a broken end ring and which belong now to the ring mesh.

SIMULATION RESULTS

Simulations are carried out using a motor which has parameters: 4 Kw, 230/400v, 14.2/8.2 A, 2840 rpm, 2 poles, 24 stator slots, 30 rotor bars. Many simulation results can be exposed here but we choose to show the alpha-beta axes currents pattern (Concordia transform) and the electromagnetic torque waveforms for the work is carried on a healthy motor first and then carried on a faulty motor.

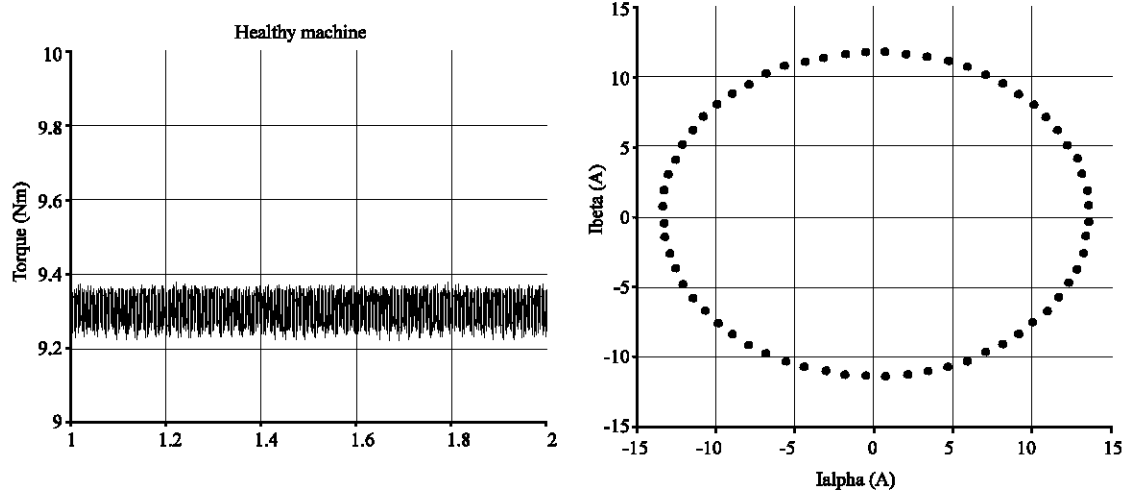


Fig. 2: Shape of electromagnetic torque and Concordia's vector pattern in the case of healthy machine

Fig. 3: Shape of electromagnetic torque and Concordia's vector pattern in the case of broken bar

In the study of healthy machine, the Concordia current components lead to an alpha-beta's vector is represented by Fig. 2 and its representation give a circular pattern centered at the origin. The presence of faulty bars is illustrated by Fig. 3 and corresponding to the breaking of two broken bar case. In the study of broken rotor bar, the Concordia's vector pattern remains circular with regular geometric forms around the main circle and the electromagnetic torque waveforms is clearly modulated by the $2sf_1$ related to the $(1 \pm 2s)f_1$ stator current harmonics. This phenomenon can be exploited by pattern recognition algorithms issued from the image processing methods.

CONCLUSION

In this study, a winding function theory based global model for the simulation of faulty induction machines under stator and rotor faults was presented. An approach based on the drawing of the Concordia current components for the monitoring of induction motor by computer is being used. However, the interest of the used technique lies in the possibility to detect bars fault in the possibility to detect bars fault by the distortion of the Concordia current components leads to an alpha-beta's vector. The inductances calculation based on magnetic energy considerations was exposed and the numerical storage of inductances was discussed. The

simulated results show that rotor cage faults can effectively detected by the proposed approach.

REFERENCES

1. Szabo, L., J.B. Dobai and K.A. Biro, 2004. Rotor faults detection in squirrel cage induction motors by current signature analysis, International Conference on Automation, Quality and Testing Robotics, Cluj-Napoca, Romania, pp: 13-15.
2. Cardoso, A.J.M., 1995. And al, Rotor cage fault diagnosis in three-phase induction motors, by Park's vector approach, 30th Ind. Applic Society Annual Meeting, Orlando, Florida, pp: 642-646.
3. Awadallah, M.A. and M.M. Morcos, Application of AI tools in fault diagnosis of electrical machines and drivers, an overview IEEE Trans Energy Convers, 18: 245-251.
4. Benbouzid, M.E.H., 2000. A review of induction motors signature analysis as a medium for faults detection, IEEE Trans. Ind. Electron., pp: 984-993.
5. Legowski, S.F., A.H.M. Sadrul Ula and A.M. Trzynadlowski, 1996. Instantaneous stator power as a medium for the signature analysis of induction motors, IEEE Trans. Ind. Applicat., pp: 904-909.
6. Hsu, J.S., 1995. Monitoring of defects in induction motors through air-gap torque observation, IEEE Trans. Ind. Applicat., pp: 1016-1021.
7. Ostovic, V., 1989. Dynamics of Saturated Electric Machines, Springer-Verlag, New York.
8. Liao, Y. and T.A. Lipo, 1994. Effect of saturation third harmonic on the induction machine performance, Elect. Mach. Power Syst., pp: 155-171.
9. Houdouin, G., G. Barakat, T. Derrey and E. Destobbeleer, 1997. A simple analytical model for the calculation of harmonics due to slotting in the airgap flux density waveform of an electrical machine, in Proc. EPE'97, Trondheim, Norway, pp: 2601-2605.
10. Benouzza, N., M. Zerikat and A. Benetton, 2006. Squirrel Cage Rotor Faults Detection In Induction motor Utilizing Advanced Park's Vectors Approach, International conference on control, Modeling and Diagnostis, Annaba, Algeria, pp: 22-24.
11. Houdouin, G., G. Barakat, B. Dakyo and E. Destobbeleer, 2001. An improved method for dynamic simulation of air-gap eccentricity in induction machines, in Proc. IEEE SDEMPED'01, Grado, Italy, pp: 133-138.
12. Houdouin, G., G. Barakat, B. Dakyo and E. Destobbeleer, 2002. A Method for the simulation of inter-turn short circuits in squirrel cage induction machines, in Proc. of EPE-PEMC'02, Cavtat and Dubrovnik, Croatia, pp: 9-11.
13. Milimonfared, J. And Al, A novel approach for broken rotor bar detection in cage induction motors, IEEE Transaction on Industry Applications, n°.5, pp: 1000-1006.